ACS Photonics

Article

pubs.acs.org/journal/apchd5

High-Order Hilbert Curves: Fractal Structures with Isotropic, Tailorable Optical Properties

Stefano De Zuani,[†] Thomas Reindl,[‡] Marcus Rommel,[‡,§] Bruno Gompf,[*,†] Audrey Berrier,[†] and Martin Dressel[†]

[†]Physikalisches Institut and Research Center SCoPE, Universität Stuttgart, Pfaffenwaldring 57, 70569 Stuttgart, Germany

[‡]Max Planck Institute for Solid State Research, Heisenbergstrasse 1, 70569 Stuttgart, Germany

Supporting Information

ABSTRACT: Fractals are promising candidates as nonperiodic, nonresonant structures exhibiting a homogeneous, isotropic, and frequency-independent effective optical response. We present a comprehensive optical investigation of a metallic Hilbert curve of fractal order $N = 9$ in the visible and near-infrared spectral range. Our experiments show that high-order fractal nanostructures exhibit a nearly frequency independent reflectance and an in-plane isotropic optical response. The response can be simulated in the framework of a simple effective medium approximation model with a limited number of parameters. It is shown that high-order Hilbert structures can be considered as a "transparent in-plane metal", the dielectric function of which is modified by the filling factor f, hence creating a tunable conductive effective metal with tailorable plasma frequency and variable reflectance without going through an insulator-to-metal transition.

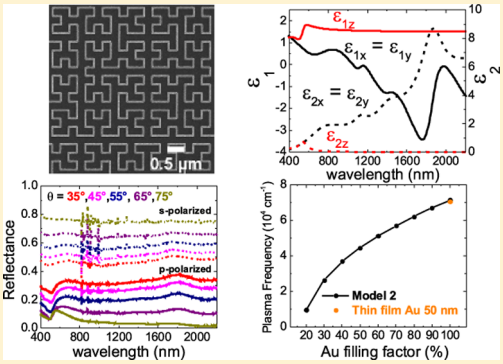

KEYWORDS: *Hilbert curve, fractal, self-similar nanostructures, optical properties, spectroscopic ellipsometry, tunable metal, Bruggeman effective medium approximation, visible, near-infrared, optical frequencies*

Most concepts for metamaterials start with a basic unit—"photonic atoms"—made of a metallic rod-based nanostructure forming a resonator. These building blocks are usually arranged in a periodic array, which is assumed to represent an isotropic effective medium with the desired optical response.[1] Due to the isolated building blocks, these structures are never metallic on a larger scale; that is, they exhibit no dc conductivity. At microwave frequencies, standard procedures were established for the design of bulk artificial media with negative effective optical parameters.[2] The disadvantage of this design concept is that such resonator structures provide the desired optical property only over a small frequency range, and the periodic arrangement leads usually to some anisotropy. In the visible and near-infrared spectral range, nanostructures made by state-of-the-art lithographic methods have the additional problem that they are not small enough compared to the wavelength. Therefore, spatial dispersion cannot be neglected, and even simple periodic nanostructures tend to exhibit a complex anisotropic polarization behavior, which cannot be described by effective parameters anymore.[3] In the case of two-dimensional periodic and conductive structures made of metallic lines in squared or crossed patterns, it is known that their optical properties are in general strongly affected by plasmonic resonances and by the diffraction modes due to the periodicity, which makes the reflectance strongly dependent on the wavelength.[4−6] Ultrathin metal films exhibit, instead, an isotropic nearly frequency-independent optical behavior, which theoretically can be tuned by their thickness. In practice, however, below a certain critical thickness, the so-called percolation threshold, they undergo a metal-to-insulator transition, where the dielectric properties diverge.[7] One way to overcome this problem is to look for continuous metal structures with a homogeneous, isotropic, and frequency-independent behavior. Self-similar structures are in fact promising candidates to fulfill these conditions and are known to foster frequency-independent properties.[8] Fractal structures exhibit additionally no long-range spatial correlations and therefore are expected to show no spatial dispersion. Some time after the discovery of fractal structures in nature,[9] the first multiband fractal antenna designs for the microwave region were suggested,[10−13] and recently metamaterials based on fractal geometries have been investigated even at optical frequencies.[14−18]

Hilbert fractal curves are self-avoiding, continuous curves, proposed for the first time by David Hilbert[19] in 1891 as a particular geometry of a family of curves introduced by Giuseppe Peano[20] in 1890, known as "FASS curves" (space-*f*illing, self-*a*voiding, *s*imple and self-similar). The simplest Hilbert curve, fractal order $N = 1$, is formed by a "U"-shaped meander line similar to a split-ring resonator (see Supporting Information). With a recursive algorithm the area is then divided into four quadrants, in each of which a smaller version

Received: June 30, 2015
Published: November 23, 2015

DOI: 10.1021/acsphotonics.5b00363
ACS Photonics 2015, 2, 1719−1724

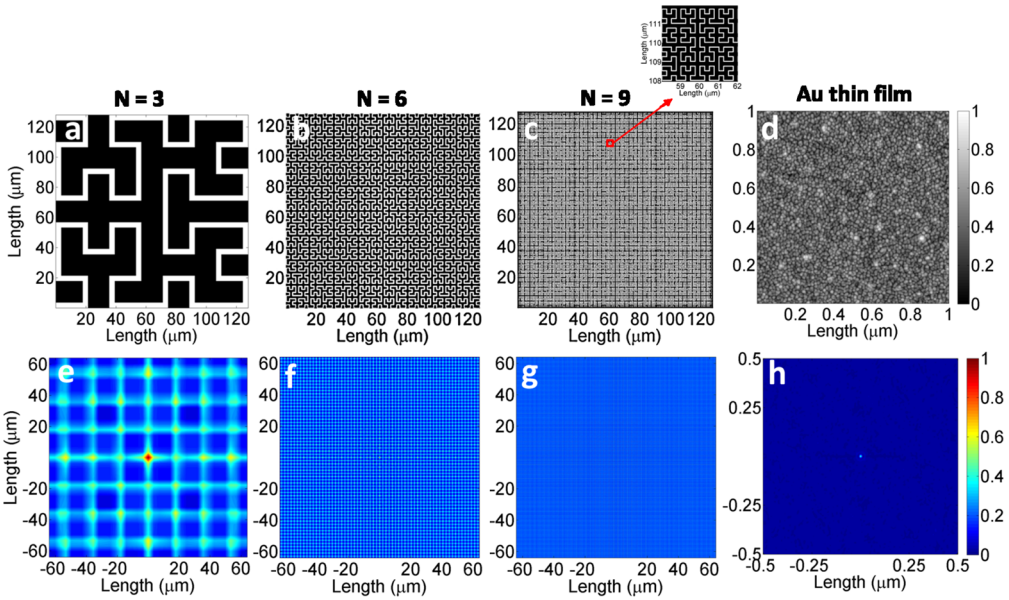

Figure 1. (a–d) Real-space Hilbert curves of fractal orders $N = 3$, 6, and 9 and atomic force microscope image of a thin gold film of 5.2 nm thickness close to the percolation threshold. The white line on the black area is the Hilbert curve. The scale bar on the right is identical for all figures. In part (c) the Hilbert curve cannot be resolved due to limitations in the pixel resolution; the inset displays a zoomed-in view of a selected area of ~4 × 4 μm^2, as indicated by the red arrow. (e–h) Corresponding autocorrelation function images. The scale bar on the right is identical for all figures.

of the precedent order is placed. The four new "U"-shaped structures are connected to form a Hilbert curve with $N = 2$. The same iteration is repeated for $N = 2$ to form a Hilbert curve with $N = 3$, shown in Figure 1a. By continuing to increase the fractal order N, the space-filling characteristic of the Hilbert curve leads to an increase of the total length of the line, resulting for large N in the filling up of the entire area. Hence, for a given total area, the higher the order N of the structure is, the longer the line is. Since the Hilbert curve is a long self-avoiding line, its topological dimension is equal to 1 independently of the fractal order N. Nevertheless, the similarity dimension DS describes how thoroughly a fractal of order N fills up the space it inhabits.[21] For common geometries such as a line, a square, and a cube the similarity dimension equals the canonical topological dimensions of 1, 2, and 3, respectively. Hilbert curves have a similarity dimension defined by a noninteger number between 1 and 2. DS increases with fractal order N until it approaches the limit of DS = 2, corresponding to the Hausdorff dimension of a Hilbert curve[22] for $N \rightarrow \infty$, for a completely filled area (i.e., a closed thin film). (See the Supporting Information.) As the similarity dimension approaches DS = 2, the Hilbert curve accomplishes a continuous mapping of the unit area onto a one-dimensional line, and it behaves as a quasi-closed surface, almost filling the area completely.[23] Although they have been known for a long time, little has been done so far to investigate the optical properties of structures based on space-filling curves at optical frequencies.[24] Hilbert structures could provide a new variety of geometrical shapes that are by definition nonperiodic. They have the advantage that spatial dispersion should be limited due to the absence of spatial correlations. Most of the optical studies up to now were restricted to low fractal orders ($N \leq 5$) and experimentally confined to intensity transmittance or reflectance measurements at normal incidence,[25] disregarding a potential k-dependence of the optical response typical for plasmonic structures.

Here, we present a comprehensive optical investigation of a metallic Hilbert nanostructure of fractal order $N = 9$ in the visible and near-infrared spectral range. To the best of our knowledge, this is the highest fractal order ever experimentally investigated. It leads to an optical response that is quasi-independent of the wavelength of the incoming light, is fully isotropic, and can be simulated by a simple set of effective optical parameters. Moreover, we show that the quasi-frequency-independent reflectivity can be modified over a large range by simply increasing the width of the Hilbert curve at constant order N while the conductive properties of the structure stay preserved. The fractal nature of the Hilbert curve allows us to fabricate a well-defined conductive path that spans from one side to the other of the sample. At the same time, the structure reaches flat reflectance, always staying well above the percolation threshold. In-plane it is metallic and out-of-plane it exhibits dielectric behavior; that is, the Hilbert structure is essentially an artificial hyperbolic material when substrate effects are additionally taken into account.[26]

It is interesting to look at the evolution of the Hilbert structure with increasing fractal order N to check from which order the Hilbert structure can be considered isotropic. Figure 1 shows the evolution of the Hilbert curve with increasing N compared with a 5.2 nm thick gold film close to the percolation threshold, Figure 1a–d, together with the corresponding autocorrelation function images, Figure 1e–h. The autocorrelation function of the Hilbert structure of fractal order $N = 3$ (Figure 1e) exhibits a periodic array of equally spaced single sharp peaks demonstrating still a quite high spatial correlation. Quasi-crystalline structures, as alternative self-similar non-periodic structures, would exhibit a similar autocorrelation function containing sharp peaks with much weaker intensities between the peaks. With increasing fractal order N from 3 to 9 these peaks become closer and closer and a much smoother autocorrelation image appears. The absence of pronounced single sharp peaks in the autocorrelation function spectra for the order $N = 9$ (Figure 1g) reflects the absence of long-range

DOI: 10.1021/acsphotonics.5b00363
ACS Photonics 2015, 2, 1719–1724

correlations for this Hilbert structure. Its autocorrelation function is as smooth as that of a totally random discontinuous Au film close to the percolation threshold (Figure 1h). The size of the atomic force image of Figure 1d is chosen as $1 \times 1\ \mu m^2$ to visualize the cluster sizes of the Au film. These clusters lead to some short-range correlations, i.e., a high Gaussian peak in the center of Figure 1h, which demonstrate that even for a random gold film some spatial correlations due to the average cluster size can be detected. In the optical properties this short-range correlation shows up in pronounced particle plasmons in the visible for Au films close to the percolation threshold.[7] In the high-order Hilbert structure even these short-range correlations are missing, and therefore the optical response is nearly flat. The absence of any long-range order is also reflected by the similarity dimension DS. Whereas for the order $N = 3$ DS = 1.694, for $N = 9$ DS = 1.994, very close to the limit DS = 2 for $N \rightarrow \infty$, i.e., a closed thin film. Therefore, it is reasonable to assume that an increase of the fractal order N does not significantly change the properties of the structure anymore. In this work, we fabricate a gold Hilbert nanostructure of order $N = 9$ by means of electron beam lithography on a silicon substrate covered with 3 nm of native oxide.[27] The Hilbert nanostructure consists of a gold wire covering an area of $130 \times 130\ \mu m^2$. The total wire length of 6.5 cm compared to the width and thickness of 50 nm gives a very large aspect ratio of the gold wire. The total patterned area is 2.6 mm by 1.3 mm, obtained by repeating 20×10 times the writing field of $130 \times 130\ \mu m^2$ (see the Supporting Information). In Figure 2 the

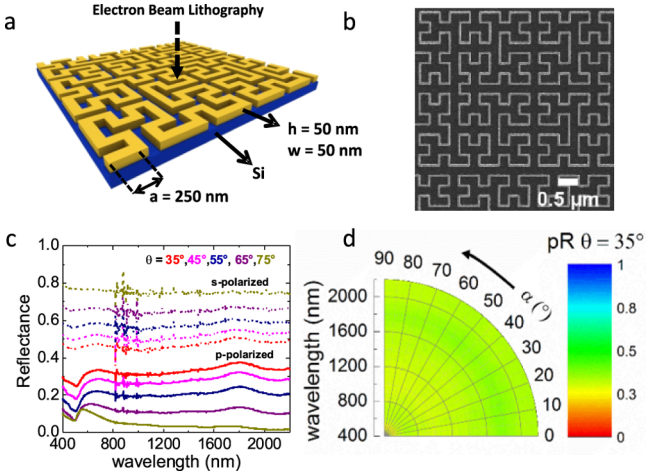

Figure 2. (a) Schematic 3D drawing of a Hilbert nanostructure. (b) Scanning electron microscope image of part of the Hilbert nanostructure of fractal order $N = 9$. (c) Experimental reflectance measured with p-polarized (solid curve) and s-polarized (dashed curve) light at an angle of incidence $\theta = 35°$ (red), 45° (magenta), 55° (navy), 65° (purple), and 75° (dark yellow). (d) Dependence of the reflectance on the azimuthal angle α measured with p-polarization at $\theta = 35°$.

structure is sketched next to a scanning electron microscope picture of an area of $5 \times 5\ \mu m^2$. The geometrical parameters lead to a gold filling factor f equal to 20% of the total area, and the shortest segment has a length a equal to 250 nm. In order to experimentally confirm the isotropic and frequency-independent response of the Hilbert structure, intensity reflectance measurements using p-polarized and s-polarized incident light were carried out with a Woollam variable-angle spectroscopic ellipsometer (WVASE) between 400 and 2200 nm, varying the angle of incidence from 30° to 75° in steps of 5°. Azimuthal-dependent measurements were also performed in the same range for p-polarized light, by rotating the sample from $\alpha = 0°$ to 90° in steps of 5° at an angle of incidence $\theta = 35°$. In Figure 2c the results show a quasi-flat reflectance over the entire frequency range, independent of the angle of incidence and polarization. The reflectance is constant within 5% by varying α, as seen in Figure 2d. The quasi-flat reflectance shown in Figure 2c is similar to the optical response of thin metallic films, which also exhibit a frequency-independent reflectivity.[7] Additionally, variable-angle spectroscopic ellipsometry measurements were performed to determine the effective optical constants of the Hilbert structure with the same experimental parameters used for the reflectance. The ellipsometry data as well as the reflectance data were subsequently modeled by a uniaxial general oscillator layer model (model 1) with in-plane isotropy on top of the substrate, which was measured and modeled separately. (See the Supporting Information.) After modeling, the real and imaginary parts of the effective dielectric functions were extracted. In the first two plots of Figure 3 the comparison

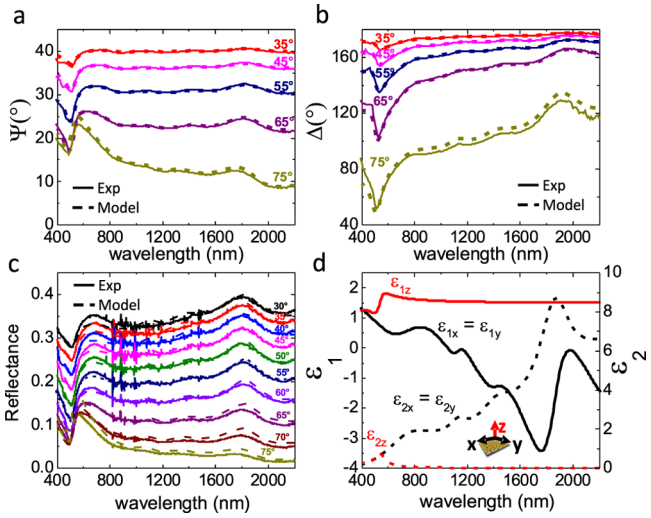

Figure 3. Experimental (solid curve) and simulated (dashed line) by model 1 spectroscopic ellipsometry angles (a) Ψ (deg) and (b) Δ (deg) for five different angles of incidence. (c) Experimental (solid curve) and simulated by model 1 (dashed curve) reflectance for 10 different angles of incidence and p-polarized light. (d) In-plane (black) and out-of-plane (red) real (solid line) and imaginary (dashed line) part of the dielectric function extracted from model 1.

between the measured spectroscopic ellipsometry angles Ψ(deg) (Figure 3a) and Δ(deg) (Figure 3b) and those extracted from model 1 is plotted for five different angles of incidence. In addition, in Figure 3c the comparison between the measured reflectance and that extracted from model 1 is plotted for p-polarized light for 10 different angles of incidence: a nearly perfect fit of the measured spectroscopic ellipsometry data and reflectance is obtained for all measured curves. The real and imaginary parts of the effective dielectric constant extracted from model 1 are shown in Figure 3d. The sample shows an in-plane metallic behavior for $\lambda \geq 1050$ nm and a nearly constant and positive out-of-plane dielectric behavior with $\varepsilon_1(\lambda)$ having positive values between 1 and 2. Metamaterials with in-plane negative components and an out-of-plane positive component of the dielectric tensor are in

DOI: 10.1021/acsphotonics.5b00363
ACS Photonics 2015, 2, 1719−1724

general identified as type II hyperbolic metamaterials.[26,28] This finding suggests that Hilbert curve based nanostructures may also be used to create very thin hyperbolic metamaterials for applications in the optical frequency range. Furthermore, the effective in-plane $\varepsilon_1(\lambda)$ has values between 0 and −4 in the near-infrared frequency range, which is also an important property for applications where low values of the negative real dielectric function are preferred (e.g., hyperlenses).[29] The in-plane imaginary part of the dielectric constant of Figure 3d increases with increasing wavelength due to the Drude component at which four distinct absorption peaks at 850, 1150, 1470, and 1870 nm are superimposed. These peaks already visible in the reflectance curve (Figure 2c) are related to resonances within the fabricated Hilbert structure due to the finite width of the gold wire.[30] The out-of-plane $\varepsilon_2(\lambda)$ of Figure 3d is zero over the whole frequency range except for the presence of a small peak at 530 nm, where the out-of-plane plasmonic resonance of the structure is present.

The measured spectroscopic ellipsometry angles Ψ (deg) and Δ (deg) and the reflectance shown in Figure 3a,b,c resemble the optical response of ultrathin Au films, except for the presence of the broad resonances previously discussed. In the next step, we therefore model the optical properties of our sample by a simple Bruggeman effective medium approximation (BEMA);[31] that is, we model it as a composite of Au and voids. In the following we call this BEMA approach, model 2. For the modeling we always stay in the metallic regime above the percolation threshold, considering the fact that our Hilbert structure always stays conductive. In model 2 (BEMA) the same out-of-plane general oscillator layer model as in model 1 is used, but the in-plane optical properties are described by a BEMA model in which the Hilbert structure is considered as an effective medium and simulated using the dielectric optical constants of a real 50 nm thick closed gold film with a filling factor f of 20% and 80% voids (see Supporting Information). The depolarization factor $L = 0.18$ is chosen as best fit and kept fixed. The comparison between the measured and simulated spectroscopic ellipsometry angles Ψ (deg) and Δ (deg) is shown in Figure 4a and b, respectively. The reflectance simulated from model 2 is compared with the measured reflectance in Figure 4c, while the simulated in-plane and out-of-plane components of the permittivity are plotted in Figure 4d. As we can see from these figures, the much simpler model 2 is in good agreement with the overall behavior of the measured data of Figure 4a−c, except for the four absorption peaks seen in Figure 3d coming from local resonances depending on the specific shape of the Hilbert structure. This agreement is interesting, because effective medium theories totally neglect the specific shape and size of the structure. It especially stresses the fact that even though the Hilbert structure is not in the limit of period/lambda ≪ 1, it can be treated as an effective medium exhibiting no k-dependence of the optical response. The good overall agreement of model 2 with the measured spectroscopic ellipsometry and reflectance data allows us to simulate the in-plane optical properties of the complex Hilbert structure by only two parameters, the depolarization factor L and the gold filling factor f, instead of the 15 free parameters (amplitude, broadening, and position for each of the oscillators) used in model 1. In the following we will use the simple model 2 to predict the evolution of the optical properties of the Hilbert structure with increasing gold coverage. We fix the order of the Hilbert structure to $N = 9$ and assume a constant depolarization factor $L = 0.18$. The only tuning parameter left is then the

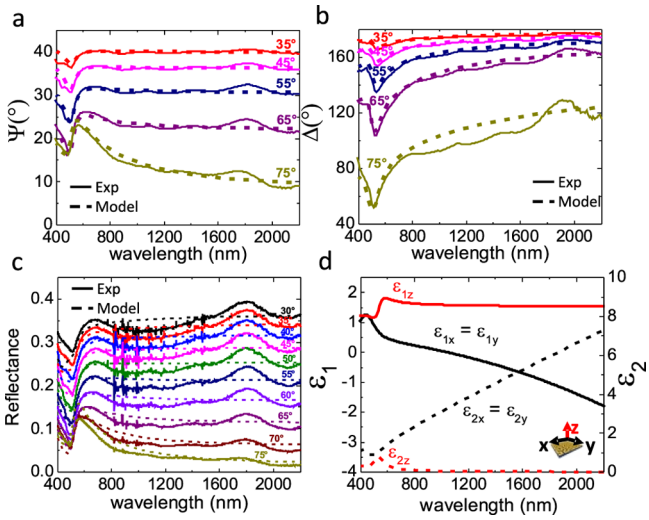

Figure 4. Experimental (solid curve) and simulated (dashed line) by model 2 spectroscopic ellipsometry angles (a) Ψ (deg) and (b) Δ (deg) for five different angles of incidence. (c) Experimental (solid curve) and simulated by model 2 (dashed curve) reflectance for 10 different angles of incidence and p-polarized light. (d) In-plane (black) and out-of-plane (red) real (solid line) and imaginary (dashed line) part of the dielectric function extracted from model 2.

width w of the wire. In model 2 increasing the width w is equivalent to increasing the gold filling factor f. As previously mentioned, model 2 does not take into account contributions from the local resonances in the Hilbert curve, which can influence the optical response of the structure. Especially at high gold filling factors f, the width w becomes comparable with the size a of the curve and reduces the gap between the individual segments of the structure, hence increasing their optical coupling and modifying the resonances. However, as a first approximation neglecting the presence of the resonances, model 2 allows us to simulate the evolution of the reflectance and of the corresponding plasma frequency with increased width w of the structure from $w = 50$ nm ($f = 20\%$, measured structure) to $w = 250$ nm ($f = 100\%$, closed gold film).

As already stated, a metallic Hilbert structure is by definition always conducting even for the lowest filling factors f, in contrast to ultrathin metallic films, which always cross a percolation threshold at some specific critical thickness. Neither varying the width w of the structure nor varying the order N of the Hilbert curve will lead to an insulator-to-metal transition; hence no limitations in the use of the BEMA model for different filling factors are present. The results of the simulation with increased gold filling factor f are shown in Figure 5. The reflectance and the corresponding plasma frequency increase gradually with the filling factor f until they reach the values of a closed pure gold film without going through a percolation threshold as in the case of a metallic thin film. The simulation clearly shows that the optical behavior of the high-order Hilbert structure, even though always metallic, can be tailored over a wide range: by only varying the width w of the curve, a broad range of plasma frequencies can be reached from the ultraviolet up to the near-infrared frequency range. In this sense, our structure represents an artificially tailored metal.

In summary, we have investigated the optical response of a metallic Hilbert nanostructure of fractal order $N = 9$ in the optical frequency range. We experimentally showed that high-order fractal structures exhibit a nearly frequency-independent

DOI: 10.1021/acsphotonics.5b00363
ACS Photonics 2015, 2, 1719−1724

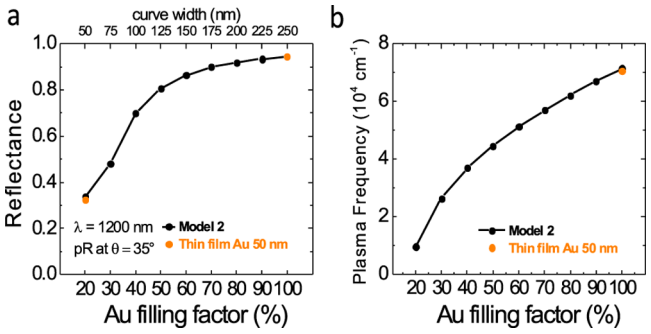

Figure 5. (a) Reflectance values at λ = 1200 nm simulated for different Au filling factors f, i.e., different width of the structure, using the BEMA model 2 for p-polarized incident radiation at θ = 35°. (b) Plasma frequency as a function of the Au filling factor f, obtained from the simulated in-plane real part of the dielectric functions fitted with the Drude formula. The orange dots in both figures are the experimental values for a closed 50 nm gold film (dots at f = 100%) and for the here investigated Hilbert structure (f = 20%), respectively.

reflectance and an isotropic in-plane optical response even though they are not in the limit period/lambda ≪ 1; the effective response can be simulated in the framework of a simple effective medium approximation model with a very limited number of parameters. Our sample shows an in-plane metallic behavior and an out-of-plane dielectric response and can be treated therefore as an artificial hyperbolic metamaterial. From the simulations we can show that high-order Hilbert structures can be considered as a "transparent in-plane metal", and their dielectric functions can be tailored through the filling factor f, hence creating a tunable conductive and effective metal with tailorable plasma frequency and variable reflectance without going through an insulator-to-metal transition.

■ ASSOCIATED CONTENT

Supporting Information

The Supporting Information is available free of charge on the ACS Publications website at DOI: 10.1021/acsphotonics.5b00363.

Design and fabrication of the Hilbert structure; details about the models described in this article; plot of the measured and simulated reflectance at normal incidence over a broad frequency range (PDF)

■ AUTHOR INFORMATION

Corresponding Author

*E-mail: b.gompf@physik.uni-stuttgart.de.

Present Address

§Chalmers University of Technology, MC2 Kemivägen 9, 41285 Gothenburg, Sweden.

Notes

The authors declare no competing financial interest.

■ ACKNOWLEDGMENTS

We acknowledge financial support by the Deutsche Forschungsgemeinschaft via DFG DR228/38-1. A.B. acknowledges the Carl Zeiss Foundation for support.

■ REFERENCES

(1) Shalaev, V. M. Transforming Light. *Science* **2008**, *322*, 5900.

(2) Smith, D. R.; Pendry, J. B.; Wiltshire, M. C. K. Metamaterials and negative refractive index. *Science* **2004**, *305*, 5685.

(3) Gompf, B.; Braun, J.; Weiss, T.; Giessen, H.; Dressel, M.; Hübner, U. Periodic nanostructures: spatial dispersion mimics chirality. *Phys. Rev. Lett.* **2011**, *106*, 185501.

(4) Oates, T. W.; Dastmalchi, B.; Isic, G.; Tollabimazraehno, S.; Helgert, C.; Pertsch, T.; Kley, E.-B.; Verschuuren, M. A.; Bergmair, I.; Hingerl, K.; Hinrichs, K. Oblique incidence ellipsometry charachterization and the substrate dependence of visible frequency fishnet metamaterials. *Opt. Express* **2012**, *20*, 11166−11177.

(5) Zhan, P.; Liu, J. B.; Dong, W.; Dong, H.; Chen, Z.; Wng, Z. L.; Zhang, Y.; Zhu, S. N.; Ming, N. B. Reflectivity behavior of two-dimensional ordered array of metallodielectric composite particles at large incidence angles. *Appl. Phys. Lett.* **2005**, *86*, 051108.

(6) Giudicatti, S.; Valsesia, A.; Marabelli, F.; Colpo, P.; Rossi, F. Plasmonic resonances in nanostructured gold/polymer surfaces by colloidal lithography. *Phys. Status Solidi A* **2010**, *207*, 935−942.

(7) Hövel, M.; Gompf, B.; Dressel, M. Dielectric properties of ultrathin metal films around percolation threshold. *Phys. Rev. B: Condens. Matter Mater. Phys.* **2010**, *81*, 035402.

(8) Werner, D. H.; Werner, P. L. Frequency-independent features of self-similar fractal antennas. *Radio Sci.* **1996**, *31*, 1331−1343.

(9) Mandelbrot, B. B. *The Fractal Geometry of Nature*; Henry Holt and Company, 1983.

(10) Puente-Baliarda, C.; Romeu, J.; Pous, R.; Cardama, A. On the behavior of the Sierpinski multiband fractal antenna. *IEEE Trans. Antennas Propag.* **1998**, *46*, 517−524.

(11) McVay, J.; Engheta, N.; Hoorfar, A. High impedance metamaterial surfaces using Hilbert curve inclusions. *IEEE Microwave Wireless Comp. Lett.* **2004**, *14*, 130−132.

(12) Best, S. R.; Morrow, J. D. The effectiveness of space-filling fractal geometry in lowering resonant frequency. *IEEE Antennas and Wireless Propagation Letters* **2002**, *1*, 112−115.

(13) Chen, R.; Li, S.; Gu, C.; Anwar, S.; Hou, B.; Lai, Y. Electromagnetic charachteristics of Hilbert curve-based metamaterials. *Appl. Phys. A: Mater. Sci. Process.* **2014**, *117*, 445−450.

(14) Gottheim, S.; Zhang, H.; Govorov, A. O.; Halas, N. J. Fractal Nanoparticles Plasmonics: The Cayley Tree. *ACS Nano* **2015**, *9*, 3284−3292.

(15) Cakmakyapan, S.; Cinel, A. N.; Cakmak, A. O.; Ozbay, E. Validation of electromagnetic field enhancement in near-infrared through Sierpinski fractal nanoantennas. *Opt. Express* **2014**, *22*, 19504−19512.

(16) Rosa, L.; Sun, K.; Juodkazis, S. Sierpinski fractal plasmonic nanoantennas. *Phys. Status Solidi RRL* **2011**, *5*, 175−177.

(17) Li, G.; Chen, X.; Ni, B.; Li, X.; Huang, L.; Jiang, Y.; Hu, W.; Lu, W. Fractal H-shaped plasmonic nanocavity. *Nanotechnology* **2013**, *24*, 205702.

(18) Volpe, G.; Volpe, G.; Quidant, R. Fractal plasmonics: subdiffraction focusing and broadband spectral response by Sierpinski nanocarpet. *Opt. Express* **2011**, *19*, 3612−3618.

(19) Hilbert, D. Über die stetige Abbildung einer Linie auf ein Flächenstück. *Mathematische Annalen* **1891**, *38*, 459−460.

(20) Peano, G. Sur une courbe, qui remplit toute une aire plane. *Mathematische Annalen* **1890**, *36*, 157−160.

(21) Peitgen, H. O.; Jürgens, H.; Saupe, D. Chaos and Fractals: New Frontiers of Science. In *Length, Area and Dimensions*; Springer: New York, 2004; pp 192−254.

(22) Sanchez-Hernandez, D. A. Multiband Integrated Antennas for 4G Terminals. In *Printed Multiband Fractal Antennas*; Artech House Inc: Boston, 2008; pp 101−125.

(23) Schroeder, M. R. Number Theory in Science and Communication. In *Self-Similarity, Fractals, Deterministic Chaos and a New State of Matter*; Springer-Verlag: Berlin, 1984; pp 326−328.

(24) Grigorenko, I. Nanostructures with the Hilbert curve geometry as surface enhanced Raman scattering substrates. *Appl. Phys. Lett.* **2013**, *103*, 043123.

(25) Afshinmanesh, F.; Curto, A. G.; Milaninia, K. M.; van Hulst, N. F.; Brongersma, M. L. Transparent metallic fractal electrodes for semiconductor devices. *Nano Lett.* **2014**, *14*, 5068−5074.

DOI: 10.1021/acsphotonics.5b00363
ACS Photonics 2015, 2, 1719−1724

(26) Poddubny, A.; Iorsh, I.; Belov, P.; Kivshar, Y. Hyperbolic Metamaterials. *Nat. Photonics* **2013**, *7*, 948−957.
(27) Rommel, M.; Nilsson, B.; Jedrasik, P.; Bonanni, V.; Dimitriev, A.; Weis, J. Sub-10nm resolution after lift-off using HSQ/PMMA double layer resist. *Microelectron. Eng.* **2013**, *110*, 123−125.
(28) Cortes, C. L.; Newman, W.; Molesky, S.; Jacob, Z. Quantum nanophotonics using hyperbolic metamaterials. *J. Opt.* **2012**, *14*, 063001.
(29) Atwater, H. A.; Boltasseva, A. Low-Loss plasmonic metamaterials. *Science* **2011**, *331*, 6015.
(30) Matteo, J. A.; Hesselink, L. Fractal extensions of near-field aperture shapes for enhanced transmission and resolution. *Opt. Express* **2005**, *13*, 636−647.
(31) Choy, T. C. *Effective Medium Theory: Principles and Applications*; University Press: Oxford, 1999.

DOI: 10.1021/acsphotonics.5b00363
ACS Photonics 2015, 2, 1719−1724